Inorganic Chemistry

pubs.acs.org/IC Article

Palladium(II) Modulation Enhances the Water Stability and Aqueous $^{99}TcO_4^-/ReO_4^-$ Removal Performance of Metal−Organic Frameworks

Xinyue Zhang, Xinyi Yang, Yinghui Xie, Xiaolu Liu, Mengjie Hao, Hui Yang,* Geoffrey I. N. Waterhouse, Shengqian Ma,* and Xiangke Wang*

Cite This: *Inorg. Chem.* 2024, 63, 16726−16732

Read Online

ACCESS | Metrics & More | Article Recommendations | Supporting Information

ABSTRACT: Improving the water stability of metal−organic frameworks (MOFs) is essential for their use in water pollution treatment and environmental remediation, though it remains technically challenging. Herein, we report a novel cationic MOF constructed with $[Th_6O_4(OH)_4(COO)_{12}]$ units and $[CoN_4{\cdot}Cl_2]$ units possessing a ftw-type topology (denoted as **1−Th-Co**). **1−Th-Co** itself exhibited poor water stability but excellent stability following a palladium(II) modulation strategy. Experimental studies reveal that Co(II) ions in **1−Th-Co** were replaced by Pd(II) ions through cation exchange in N,N-diethylformamide (yielding **1−Th-Pd**). The planar PdN_4 units in **1−Th-Pd** were responsible for improving the water stability of the framework. As a result, **1−Th-Pd** offered excellent stability, fast adsorption kinetics, and high removal ratios for $^{99}TcO_4^-$ and ReO_4^- (as a $^{99}TcO_4^-$ surrogate) in contaminated water. When used in packed columns, **1−Th-Pd** can dynamically capture ReO_4^- from groundwater. This work provides a new avenue for improving the water stability of MOFs, offering new vistas for the decontamination of aqueous solutions containing $^{99}TcO_4^-$ and ReO_4^-.

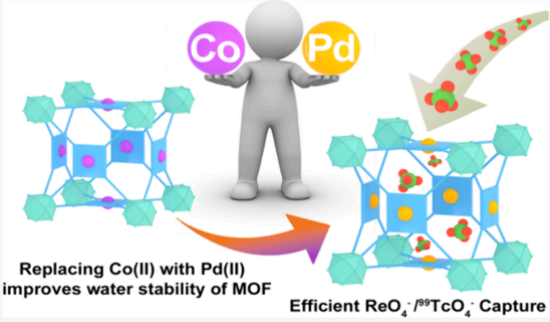

INTRODUCTION

As a structurally diverse family of crystalline porous materials, metal−organic frameworks (MOFs) nowadays find widespread application in catalysis,[1−4] gas storage and gas separation,[5−10] sensing,[11−14] uranium extraction from seawater,[15,16] environmental remediation,[17−19] and extraction metals for nuclear industry,[20] among others. MOFs can also be used as adsorbents for metal ion removal from contaminated water resources.[21−25] However, instability in water is a limitation of many MOFs, since water molecules can coordinate to metal nodes in MOFs and replace the organic linkers, thus leading to structural collapse.[26−30] Various efforts have been made to improve the water stability of the MOFs. Zhang et al. able to improve the water stability of MOF-5, HKUST-1, and ZnBT by coating a thin layer of hydrophobic polydimethysiloxane on the surface of MOF nanocrystals.[31] Other hydrophobic polymers, such as fluorine-rich and Si-based polymers, have been explored as waterproof layers to produce water-stable MOFs.[32,33] However, the drawback of using hydrophobic polymer coating strategies is that they hinder contact with target metal ions in water, thus lowering the adsorption kinetics, adsorption capacities, and (or) adsorption selectivity. Alternatively, another common approach is the direct synthesis of Zr cluster-based MOFs, which possess very strong binding affinity between Zr and organic linkers.[34−39] However, most of the reported water-stable Zr-based MOFs are neutral frameworks, rendering them unsuitable for the capture of metal cations or metal-containing anions from water solutions.

Taking the above into account, the key to resolving the water instability of MOFs lies in improving the binding affinity between metal nodes and organic linkers, while decreasing metal node-water coordination ability. Furthermore, designing MOFs with specific pore dimensions and chemical characteristics can enable the selective adsorption of target metal ions from an aqueous solution. Herein, we present a general and effective approach for improving the water stability of MOFs, involving using a facile palladium(II) modulation strategy to improve the water stability of a Th/Co bimetallic MOF. First, **1−Th-Co** with dodecahedral $[Th_6O_4(OH)_4(COO)_{12}]$ units and octahedral $[CoN_4{\cdot}Cl_2]$ units was synthesized through a solvothermal approach (Figure 1a−c). **1−Th-Co** gradually lost its crystallinity when immersed in water. Fortunately, the $[CoN_4{\cdot}Cl_2]$ units could be replaced by PdN_4 units through a cation exchange process, which generated a Th/Pd bimetallic MOF (denoted as **1−Th-Pd**). **1−Th-Pd** crystals were not accessible via the direct reaction of Pd and Th metal precursors

Received: May 22, 2024
Revised: June 28, 2024
Accepted: July 9, 2024
Published: July 20, 2024

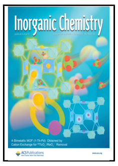

https://doi.org/10.1021/acs.inorgchem.4c02119
Inorg. Chem. 2024, 63, 16726−16732

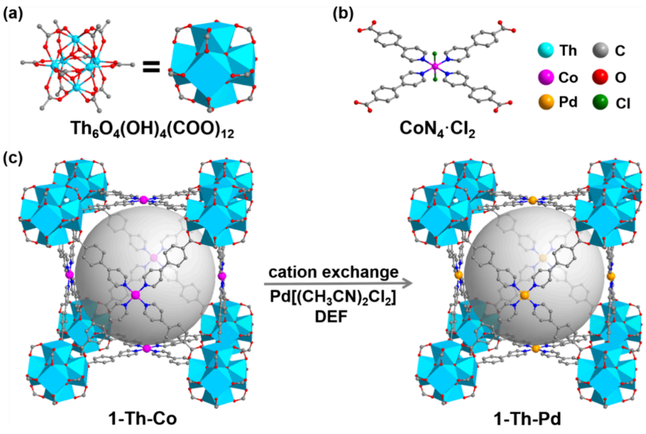

Figure 1. (a) $Th_6O_4(OH)_4(CO_2)_{12}$ unit. (b) Coordination environment of $CoN_4\cdot Cl_2$ unit. (c) Single open frameworks of **1−Th-Co** and **1−Th-Pd**, with the latter being synthesized by replacement of [$CoN_4\cdot Cl_2$] units with PdN_4 units. Cl atoms were omitted for clarity in (c).

under solvothermal conditions but were readily obtained via the ion exchange route (Figure 1c). **1−Th-Pd** showed excellent water stability in an aqueous solution. Notably, the cationic framework **1−Th-Pd** can rapidly remove low concentrations of $^{99}TcO_4^-$ and ReO_4^- (the nonradioactive analog of $^{99}TcO_4^-$) from aqueous solutions. Insights from this study can be generalized to a variety of Pd-based MOFs, providing new avenues to improve the water stability of MOFs.

MATERIAL AND METHODS

Synthesis of 1−Th-Co. A mixture of $Th(NO_3)_4\cdot xH_2O$ (0.1 mmol, 58.8 mg), $CoCl_2\cdot 6H_2O$ (0.2 mmol, 47.6 mg), 4-pyridine-4-hydroxybenzoic acid (INB) (0.3 mmol, 59.8 mg), and 20 μL of 68% HNO_3 in N,N-dimethylformamide (DMF, 5 mL) were sealed in a 25 mL glass bottle. The bottle was heated at 120 °C for 24 h under autogenous pressure and then cooled to room temperature under ambient conditions. Pink crystals were obtained and were washed with DMF.

Synthesis of 1−Th-Pd. Crystals of **1−Th-Co** (25 mg) were immersed in 5 mL of a N,N-diethylformamide (DEF) solution containing $Pd[(CH_3CN)_2Cl_2]$ (20 mg), and the resulting mixture slowly stirred at room temperature for 21 h under a N_2 atmosphere. Golden yellow crystals were obtained and washed with DEF to remove excess Pd(II).

^{99}TCO$_4^-$ AND REO$_4^-$ ADSORPTION EXPERIMENTS

Caution! ^{99}Tc is a β-emitter (E_{max} = 0.29 MeV). All operations relating to the handling of this substance were performed in a licensed radiochemical laboratory.

$^{99}TcO_4^-/ReO_4^-$ Adsorption Studies. Adsorption experiments were carried out at a fixed adsorbent/liquid ratio of 1 g/L at 25 °C. **1−Th-Pd** was dispersed in a solution containing ∼5 ppm of $^{99}TcO_4^-$. Aliquots were collected at regular time intervals while constantly stirring the dispersion. The adsorbent was collected on a 0.22 μm membrane filter, and $^{99}TcO_4^-$ in the filtrate was quantified using a liquid scintillation counting (LSC) system. A solution containing ∼10 ppm of ReO_4^- was used to verify the $^{99}TcO_4^-$ uptake results, with the ReO_4^- concentration in the filtrate quantified spectrophotometrically at 396 nm following reaction with the chromogenic agents KSCN and $SnCl_2\cdot 2H_2O$ (chromogenic method). The adsorption experiments in ∼1 ppm ReO_4^- solution and ∼5 ppm groundwater solution (as a proxy for $^{99}TcO_4^-$) were carried out under similar conditions. The concentrations of ReO_4^- were determined by ICP−MS (∼1 ppm of ReO_4^- solution) and chromogenic method (∼5 and ∼10 ppm of ReO_4^- solution).

Reusability Study. After ReO_4^- adsorption experiments (∼5 ppm), **1−Th-Pd** was immersed in 10 mL of a saturated NaCl solution at 25 °C overnight, followed by washing with distilled water. Then, the **1−Th-Pd** was subsequently returned to an aqueous solution containing ∼5 ppm of ReO_4^- for further adsorption tests.

Dynamic ReO_4^- Adsorption Studies. ReO_4^- breakthrough experiments were conducted by using a laboratory-

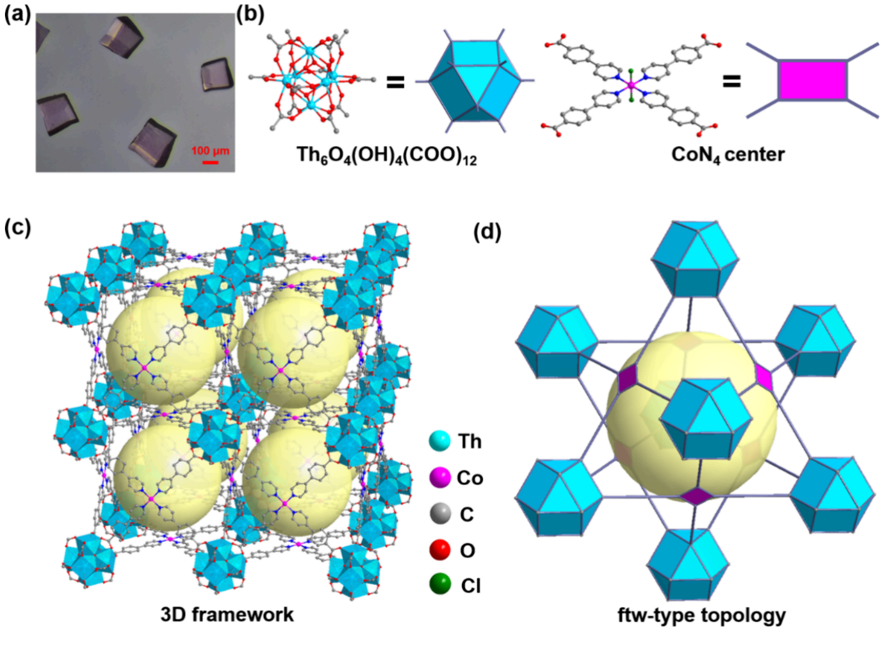

Figure 2. (a) Photograph of crystals of **1−Th-Co**. (b) View of the dodecahedral $Th_6O_4(OH)_4(CO_2)_{12}$ unit and quadrilateral CoN_4 unit. (c) 3D framework of **1−Th-Co**. (d) Topological representation of ftw nets. Cl atoms were omitted for clarity in parts (b−d).

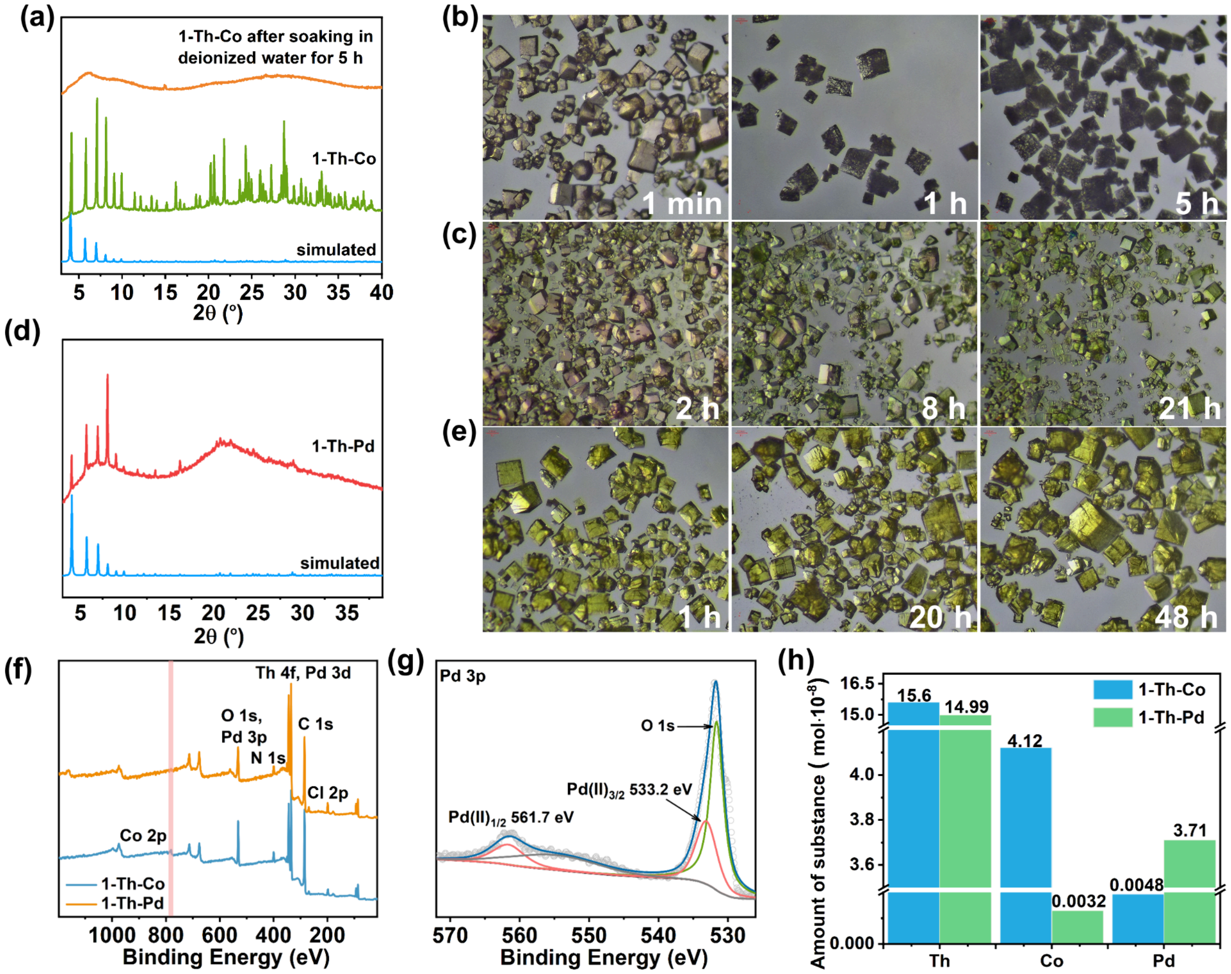

Figure 3. (a) PXRD patterns of **1−Th-Co**. (b) Photographs of **1−Th-Co** crystals in deionized water. (c) Photographs of **1−Th-Co** in a Pd[$(CH_3CN)_2Cl_2$]/DEF solution during ion exchange. (d) PXRD patterns of **1−Th-Pd**. (e) Photographs of **1−Th-Pd** in deionized water. (f) XPS survey spectra for **1−Th-Co** and **1−Th-Pd**. (g) Pd 3p XPS spectrum of **1−Th-Pd**. (h) ICP-MS analyses of **1−Th-Co** and **1−Th-Pd** showing that the molar ratio of Pd:Th in **1−Th-Pd** was 1:4 after the ion exchange step.

scale fixed-bed reactor at 25 °C. **1−Th-Pd** (100 mg) was packed into a quartz column (3.4 mm inside diameter, 1.6 mm wall thickness, 102 mm length) with degreased cotton wool filling the void space. Next, ReO_4^- spiked groundwater (~5 ppm) was flowed through the adsorbent column. The effluent from the adsorbent column was quantified by a chromogenic method. Under similar test conditions, degreased cotton wool was used as a blank for comparison.

RESULTS AND DISCUSSION

Synthesis and Characterization of MOFs. The **1−Th-Co** was synthesized via the reaction of $Th(NO_3)_4{\cdot}xH_2O$, $CoCl_2{\cdot}6H_2O$, and 4-pyridine-4-hydroxybenzoic acid (INB) in a solvent mixture of DMF and HNO_3 at 120 °C for 24 h. This yielded pink cubic crystals (Figure 2a). X-ray crystallography (SCXRD) showed that **1−Th-Co** crystallizes in the cubic space group $P\bar{4}3m$ (Table S1). One prominent structural feature of **1−Th-Co** is the presence of two kinds of metal units, including a $[Th_6O_4(OH)_4(COO)_{12}]$ unit and an octahedral Co(II) unit (Figure 2b). The $[Th_6O_4(OH)_4(COO)_{12}]$ unit acts as a single node and binds to oxygen atoms of four μ_3-O, four μ_3−OH, and 12 carboxyl groups on the INB linkers. Each octahedral Co(II) unit is coordinated by the nitrogen atoms of four pyridine rings and two chloride atoms (Figure 2b). It is interesting to note that eight $[Th_6O_4(OH)_4(COO)_{12}]$ units and six $[Co(II)N_4]$ units are connected together by 24 INB ligands into a cavity which can be filled by a ball with a diameter of 7 Å (Figure 2c). Each face of the cavity is commonly shared with an adjacent cavity to form a cationic three-dimensional framework with a ftw-type topology (Figure 2c,d). These cationic cavities are permanently porous and capable of binding anions such as $^{99}TcO_4^-$ and ReO_4^- with rapid adsorption kinetics.

Powder X-ray diffraction (PXRD) confirmed the bulk purity of **1−Th-Co** (Figure 3a). Thermogravimetric analysis (TGA) demonstrated that the framework was stable up to ~300 °C (Figure S1). The crystallinity of **1−Th-Co** gradually disappeared upon immersing the sample in aqueous solution (Figure 3b). PXRD further confirmed this collapse by the disappearance of all of the diffraction peaks (Figure 3a). Similar to $[Zr_6O_4(OH)_4(COO)_{12}]$ units, $[Th_6O_4(OH)_4(COO)_{12}]$ units are generally stable toward water. However, the $[Co(II)N_4]$ unit is prone to decomposition by water.[26] This prompted us to try and stabilize the cavity-based framework by replacing the $[Co(II)N_4]$ unit with other more water-tolerant metal-containing units.

We noticed that the introduction of planar $[Pd(II)N_4]$ units can dramatically improve the stability of MOFs in water.[33] A new heterometallic framework with Th and Pd centers was obtained after soaking **1−Th-Co** in a mixture of Pd-$[(CH_3CN)_2Cl_2]$/DEF for 21 h. As shown in Figures 1c and 3c, the original pink color of **1−Th-Co** gradually transformed to green over 8 h, with golden yellow crystal obtained as the soaking time increased up to 21 h (yielding **1−Th-Pd**). SCXRD and PXRD data revealed that the framework of **1−Th-Pd** was isomorphous to **1−Th-Co**, with unit cell parameters of $a = b = c = 21.73$ Å, $\alpha = \beta = \gamma = 90°$ (Figure 3d, Table S1). The complete substitution of Co with Pd was verified by X-ray photoelectron spectroscopy (XPS), with the Co signals being replaced with Pd signals (Figure 3f). Since Pd 3d XPS signals overlap with the Th 4f peaks, we used the Pd 3p spectrum to investigate the valence state of palladium in **1−Th-Pd**. The Pd 3p spectrum showed peaks at 533.2 and 561.7 eV, in a 2:1 area ratio, which could readily be assigned to the Pd $3p_{3/2}$ and Pd $3p_{1/2}$ signals, respectively, of a Pd(II) species (Figure 3g).[40,41] Furthermore, inductively coupled plasma mass spectrometry (ICP-MS) analyses showed that the Pd:Th molar ratio was 1:4, identical to the Co:Th ratio of 1:4 in the parent **1−Th-Co** framework, further confirming the success of the ion exchange process (Figure 3h). **1−Th-Pd** exhibited similar thermal stability to **1−Th-Co** with heating under a N_2 atmosphere (Figure S1). We further evaluated the chemical stability of **1−Th-Pd** by soaking the MOF crystals in deionized water. The photographs revealed that the crystalline structure of the MOF was retained after 48 h with no obvious structural collapse (Figure 3e). Spurred on by this success, we further conducted a series of detailed experiments to assess the anionic radionuclide adsorption performance of **1−Th-Pd**.

■ $^{99}TCO_4^-$ AND REO_4^- UPTAKE PROPERTIES

The nuclear energy industry has the potential to cause many environmental problems. Leakage of radionuclides such as $^{99}TcO_4^-$ from incorrectly stored nuclear wastes can penetrate the underground and contaminate groundwater. Due to its high water-solubility and noncomplexation, $^{99}TcO_4^-$ can be easy to spread into the environment, leading to threats to fragile ecosystems and human health.[42−45] Therefore, it is of great importance to eliminate $^{99}TcO_4^-$ from contaminated water. An adsorbent-to-liquid ratio of **1−Th-Pd** was determined to be 1 g/L, which was used for further adsorption studies (Figure S2). The $^{99}TcO_4^-$ adsorption ability of **1−Th-Pd** was first examined in NH_4TcO_4 solutions at an adsorbent-to-solution ratio of 1 g/L. As expected, **1−Th-Pd** demonstrated fast adsorption kinetics, achieving an equilibrium removal percentage of >93.7% in a ∼ 5 ppm $^{99}TcO_4^-$ solution (Figure 4a). Due to the scarcity, limited availability, and radioactivity of $^{99}TcO_4^-$, ReO_4^- as a nonradioactive surrogate with identical charge density and similar anion exchange properties was used for subsequent adsorption studies.[25,46−52] Adsorption experiments using **1−Th-Pd** were conducted in a ∼ 10 ppm ReO_4^- aqueous solution. As shown in Figure 4a, the adsorption kinetics for ReO_4^- were almost identical to those of $^{99}TcO_4^-$ under the same conditions. Further, **1−Th-Pd** can effectively remove ∼100% of ReO_4^- from ∼1 ppm of polluted water (Figure 4b). On the basis of these results, we subsequently performed adsorption experiments in ReO_4^--contaminated groundwater and tap water. **1−Th-Pd** is able to remove ReO_4^- (∼5 ppm) to the drinking water level (0 ppb) within 30 s in groundwater (Figure 4c). Moreover, the removal ratio of **1−Th-Pd** reached ∼80% in ∼5 ppm of ReO_4^--contaminated tap water (Figure S3). Next, dynamic ReO_4^- capture breakthrough experiments were performed from contaminated groundwater using **1−Th-Pd**-packed columns. As shown in Figure 4d, **1−Th-Pd** can effectively remove ReO_4^- from groundwater under slow column elution conditions (0.2 mL/min), reaching equilibrium after ∼150 min. The calculated dynamic adsorption capacity was ∼1.42 mg/g. Notably, **1−Th-Pd** exhibited an efficient dynamic ReO_4^- capture performance even at very low concentrations of ReO_4^-, indicating that it is a promising adsorbent for practical removal of $^{99}TcO_4^-$ from contaminated water sources. The FT-IR spectrum of used **1−Th-Pd** showed a new signal at 906 cm^{-1} after the adsorption experiments,[53,54] indicating that the Cl^- ions in **1−Th-Pd** were successfully exchanged by ReO_4^- ions (Figure 4e). The adsorption capacity of **1−Th-Pd** showed almost no decrease over four cycles in ∼5 ppm of ReO_4^- solutions, confirming good sorbent durability (Figure 4f). Photographs confirmed that **1−Th-Pd** maintained its crystallinity after the ReO_4^- adsorption experiments (Figures S4−S6).

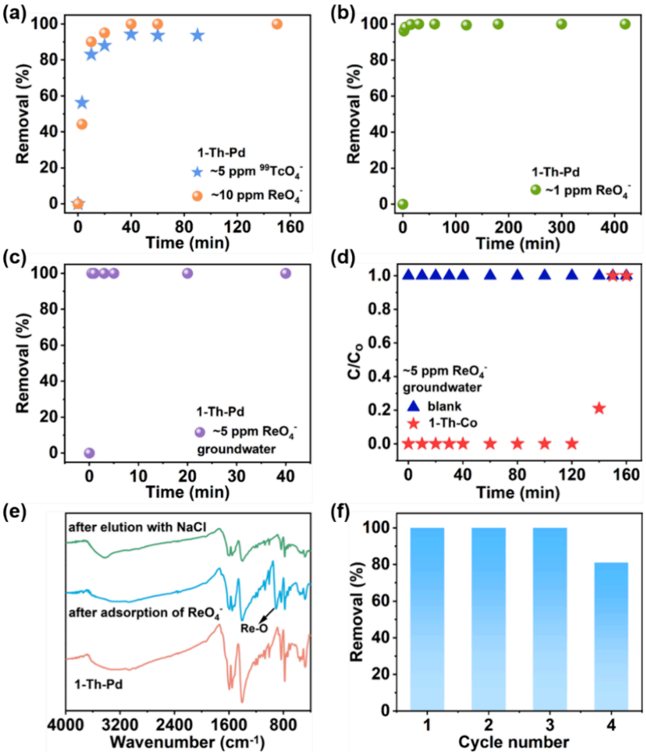

Figure 4. (a) $^{99}TcO_4^-$ and ReO_4^- adsorption kinetics on **1−Th-Pd** at initial $^{99}TcO_4^-$ and ReO_4^- concentrations of ∼5 and ∼10 ppm, respectively. (b) ReO_4^- adsorption kinetics on **1−Th-Pd** in ∼1 ppm of ReO_4^- solution. (c) ReO_4^- adsorption kinetics on **1−Th-Pd** in ∼5 ppm of ReO_4^- contaminated groundwater. (d) Experimental column breakthrough curves for ReO_4^- spiked groundwater in an absorber bed packed with **1−Th-Pd**. (e) FT-IR spectra of **1−Th-Pd** before and after adsorption of ReO_4^- and after elution with a saturated NaCl solution. (f) Recycle test data for ReO_4^- removal in groundwater.

Considering the aforementioned findings, it can be concluded that the Pd(II) exchange strategy introduced herein successfully modified a water-unstable framework **1−Th-Co** into an extremely water-stable framework **1−Th-Pd**. In comparison to $Co(II)N_4$ units, we established that the $Pd(II)N_4$ unit is resistant to moisture, therefore improving the stability of the MOF framework. We expect this finding will be of considerable interest to the MOF community. The adsorption of $ReO_4^-/^{99}TcO_4^-$ relies on cationic MOFs with high water stability, with our water-stable **1−Th-Pd** MOF likely to be suitable for the selective extraction of $ReO_4^-/^{99}TcO_4^-$ from contaminated and wastewater.

■ CONCLUSIONS

In conclusion, we have designed and synthesized a Th/Pd bimetallic MOF (**1−Th-Pd**), isoreticular to the Th/Co MOF (**1−Th-Co**) through ion exchange methods. Due to the moisture resistant performance of both the $[Th_6O_4(OH)_4(COO)_{12}]$ units and $[PdN_4]$ units, **1−Th-Pd** showed outstanding water stability. Benefiting from a cationic framework, extraordinary water stability, and a porous structure, **1−Th-Pd** displayed fast adsorption kinetics and ~100% $^{99}TcO_4^-/ReO_4^-$ removal capacity at low concentrations (~1 and ~5 ppm) in contaminated water. This study conclusively demonstrates an effective design strategy for the generation of functional MOFs with high water stability for the selective removal of target anions from aqueous solutions.

■ ASSOCIATED CONTENT

Supporting Information

The Supporting Information is available free of charge at https://pubs.acs.org/doi/10.1021/acs.inorgchem.4c02119.

> Additional experimental details, crystal structures, TGA curves, ReO_4^- removal performance, and photographs after ReO_4^- removal tests (PDF)

Accession Codes

CCDC 2354278−2354279 contain the supplementary crystallographic data for this paper. These data can be obtained free of charge via www.ccdc.cam.ac.uk/data_request/cif, or by emailing data_request@ccdc.cam.ac.uk, or by contacting The Cambridge Crystallographic Data Centre, 12 Union Road, Cambridge CB2 1EZ, UK; fax: +44 1223 336033.

■ AUTHOR INFORMATION

Corresponding Authors

Hui Yang − *College of Environmental Science and Engineering, North China Electric Power University, Beijing 102206, P. R. China*; Email: h.yang@ncepu.edu.cn

Shengqian Ma − *Department of Chemistry, University of North Texas, Denton, Texas 76201, United States*; orcid.org/0000-0002-1897-7069; Email: shengqian.ma@unt.edu

Xiangke Wang − *College of Environmental Science and Engineering, North China Electric Power University, Beijing 102206, P. R. China*; orcid.org/0000-0002-3352-1617; Email: xkwang@ncepu.edu.cn

Authors

Xinyue Zhang − *College of Environmental Science and Engineering, North China Electric Power University, Beijing 102206, P. R. China*

Xinyi Yang − *College of Environmental Science and Engineering, North China Electric Power University, Beijing 102206, P. R. China*

Yinghui Xie − *College of Environmental Science and Engineering, North China Electric Power University, Beijing 102206, P. R. China*

Xiaolu Liu − *College of Environmental Science and Engineering, North China Electric Power University, Beijing 102206, P. R. China*

Mengjie Hao − *College of Environmental Science and Engineering, North China Electric Power University, Beijing 102206, P. R. China*

Geoffrey I. N. Waterhouse − *School of Chemical Sciences, The University of Auckland, Auckland 1142, New Zealand*; orcid.org/0000-0002-3296-3093

Complete contact information is available at: https://pubs.acs.org/10.1021/acs.inorgchem.4c02119

Author Contributions

The manuscript was written through contributions of all authors. All authors have given approval to the final version of the manuscript.

Notes

The authors declare no competing financial interest.

■ ACKNOWLEDGMENTS

We gratefully acknowledge funding support from the National Science Foundation of China (Grants U2167218; 22006036), the Beijing Outstanding Young Scientist Program (H.Y. and X.W.), and the Robert A. Welch Foundation (B-0027) (S.M.). G.I.N.W. acknowledges funding support from the MacDiarmid Institute for Advanced Materials and Nanotechnology.

■ REFERENCES

(1) Kung, C. W.; Goswami, S.; Hod, I.; Wang, T. C.; Duan, J.; Farha, O. K.; Hupp, J. T. Charge Transport in Zirconium-Based Metal-Organic Frameworks. *Acc. Chem. Res.* **2020**, *53* (6), 1187−1195.

(2) Tu, Y.; Li, H.; Tu, T.; Zhang, Q. Lamellar Enzyme-Metal−Organic Framework Composites Enable Catalysis on Large Substrates. *CCS Chem.* **2022**, *4* (3), 872−879.

(3) Wang, Y.; Yan, L.; Dastafkan, K.; Zhao, C.; Zhao, X.; Xue, Y.; Huo, J.; Li, S.; Zhai, Q. Lattice Matching Growth of Conductive Hierarchical Porous MOF/LDH Heteronanotube Arrays for Highly Efficient Water Oxidation. *Adv. Mater.* **2021**, *33* (8), No. e2006351.

(4) Wei, Y. S.; Zhang, M.; Zou, R.; Xu, Q. Metal-Organic Framework-Based Catalysts with Single Metal Sites. *Chem. Rev.* **2020**, *120* (21), 12089−12174.

(5) Yang, S.-Q.; Hu, T.-L.; Chen, B. Microporous Metal-Organic Framework Materials For Efficient Capture And Separation of Greenhouse Gases. *Sci. China Chem.* **2023**, *66* (8), 2181−2203.

(6) Fan, W.; Wang, X.; Zhang, X.; Liu, X.; Wang, Y.; Kang, Z.; Dai, F.; Xu, B.; Wang, R.; Sun, D. Fine-Tuning the Pore Environment of the Microporous Cu-MOF for High Propylene Storage and Efficient Separation of Light Hydrocarbons. *ACS Cent. Sci.* **2019**, *5* (7), 1261−1268.

(7) Li, X.; Liu, J.; Zhou, K.; Ullah, S.; Wang, H.; Zou, J.; Thonhauser, T.; Li, J. Tuning Metal-Organic Framework (MOF) Topology by Regulating Ligand and Secondary Building Unit (SBU) Geometry: Structures Built on 8-Connected M_6 (M = Zr, Y) Clusters and a Flexible Tetracarboxylate for Propane-Selective Propane/Propylene Separation. *J. Am. Chem. Soc.* **2022**, *144* (47), 21702−21709.

(8) Wang, W.; Xiong, X. H.; Zhu, N. X.; Zeng, Z.; Wei, Z. W.; Pan, M.; Fenske, D.; Jiang, J. J.; Su, C. Y. A Rare Flexible Metal-Organic Framework Based on a Tailorable Mn_8-Cluster Showing Smart Responsiveness to Aromatic Guests and Capacity for Gas Separation. *Angew. Chem., Int. Ed.* **2022**, *61* (26), No. e202201766.

(9) Wang, Q.; Hu, J.; Yang, L.; Zhang, Z.; Ke, T.; Cui, X.; Xing, H. One-Step Removal of Alkynes and Propadiene from Cracking Gases Using A Multi-Functional Molecular Separator. *Nat. Commun.* **2022**, *13* (1), 2955.

(10) Ye, Z.-M.; Zhang, X.-F.; Liu, D.-X.; Xu, Y.-T.; Wang, C.; Zheng, K.; Zhou, D.-D.; He, C.-T.; Zhang, J.-P. A Gating Ultramicroporous Metal-Organic Framework Showing High Adsorption Selectivity, Capacity and Rate for Xylene Separation. *Sci. China Chem.* **2022**, *65* (8), 1552−1558.

(11) Chang, L.-M.; Zhai, R.; Ma, Z.-Z.; Huang, J.-D.; Gu, Z.-G.; Zhang, J. Liquid-Phase Epitaxial Layer by Layer Brushing Fabrication of Metal-Organic Frameworks Films. *Nano Res.* **2024**, *17*, 5698−5704.

(12) Gui, B.; Liu, X.; Yu, G.; Zeng, W.; Mal, A.; Gong, S.; Yang, C.; Wang, C. Tuning of Förster Resonance Energy Transfer in Metal−Organic Frameworks: Toward Amplified Fluorescence Sensing. *CCS Chem.* **2021**, *3* (8), 2054−2062.

(13) Lu, H.; Xie, J.; Wang, X. Y.; Wang, Y.; Li, Z. J.; Diefenbach, K.; Pan, Q. J.; Qian, Y.; Wang, J. Q.; Wang, S.; Lin, J. Visible Colorimetric Dosimetry of UV and Ionizing Radiations By A Dual-Module Photochromic Nanocluster. *Nat. Commun.* **2021**, *12* (1), 2798.

(14) Lu, H.; Hou, H.; Hou, Y.-C.; Zheng, Z.; Ma, Y.; Zhou, Z.; Guo, X.; Pan, Q.-J.; Wang, Y.; Qian, Y.; Wang, J.-Q.; Lin, J. A New Concept of Radiation Detection Based on a Fluorochromic and Piezochromic Nanocluster. *J. Am. Chem. Soc.* **2022**, *144* (8), 3449−3457.

(15) Liu, T.; Tang, S.; Wei, T.; Chen, M.; Xie, Z.; Zhang, R.; Liu, Y.; Wang, N. Defect-Engineered Metal-Organic Framework with Enhanced Photoreduction Activity toward Uranium Extraction from Seawater. *Cell Rep. Phys. Sci.* **2022**, *3* (5), No. 100892.

(16) Yang, H.; Liu, Y.; Chen, Z.; Waterhouse, G. I. N.; Ma, S.; Wang, X. Emerging Technologies for Uranium Extraction from Seawater. *Sci. China Chem.* **2022**, *65* (12), 2335−2337.

(17) Chen, Z.; Li, Y.; Cai, Y.; Wang, S.; Hu, B.; Li, B.; Ding, X.; Zhuang, L.; Wang, X. Application of Covalent Organic Frameworks and Metal−Organic Frameworks Nanomaterials in Organic/Inorganic Pollutants Removal from Solutions through Sorption-Catalysis Strategies. *Carbon Res.* **2023**, *2* (1), 8.

(18) Bobbitt, N. S.; Mendonca, M. L.; Howarth, A. J.; Islamoglu, T.; Hupp, J. T.; Farha, O. K.; Snurr, R. Q. Metal-organic Frameworks for the Removal of Toxic Industrial Chemicals and Chemical Warfare Agents. *Chem. Soc. Rev.* **2017**, *46* (11), 3357−3385.

(19) Xu, L.; Zhang, D.; Ma, F.; Zhang, J.; Khayambashi, A.; Cai, Y.; Chen, L.; Xiao, C.; Wang, S. Nano-MOF$^+$ Technique for Efficient Uranyl Remediation. *ACS. Appl. Mater. Interfaces* **2019**, *11* (24), 21619−21626.

(20) Zhao, F.; Yu, K.; Shu, K.; Su, L.; He, P.; Ma, G.; Tang, Z.; Peng, H.; Li, Y.; Ma, L. P507-modified Magnetic Porous Carbon Derived from Metal-Organic Frameworks for Efficient Separation of Zirconium(IV) and Hafnium(IV). *Sep. Purif. Technol.* **2024**, *345*, No. 127276.

(21) Shen, N.; Yang, Z.; Liu, S.; Dai, X.; Xiao, C.; Taylor-Pashow, K.; Li, D.; Yang, C.; Li, J.; Zhang, Y.; Zhang, M.; Zhou, R.; Chai, Z.; Wang, S. $^{99}TcO_4^-$ Removal from legacy Defense Nuclear Waste by An Alkaline-Stable 2D Cationic Metal Organic Framework. *Nat. Commun.* **2020**, *11* (1), 5571.

(22) Tian, J.; Shi, C.; Xiao, C.; Jiang, F.; Yuan, D.; Chen, Q.; Hong, M. Introduction of Flexibility into a Metal−Organic Framework to Promote Hg(II) Capture through Adaptive Deformation. *Inorg. Chem.* **2020**, *59* (24), 18264−18275.

(23) Li, L.-L.; Feng, X.-Q.; Han, R.-P.; Zang, S.-Q.; Yang, G. Cr(VI) Removal via Anion Exchange on a Silver-triazolate MOF. *J. Hazard. Mater.* **2017**, *321*, 622−628.

(24) Mei, D.; Liu, L.; Yan, B. Adsorption of Uranium (VI) by Metal-organic Frameworks and Covalent-organic Frameworks from Water. *Coord. Chem. Rev.* **2023**, *475*, No. 214917.

(25) Kang, K.; Liu, S. T.; Zhang, M. Y.; Li, L.; Liu, C. Y.; Lei, L. C.; Dai, X.; Xu, C.; Xiao, C. L. Fast Room-Temperature Synthesis of an Extremely Alkaline-Resistant Cationic Metal-Organic Framework for Sequestering TcO_4^- with Exceptional Selectivity. *Adv. Funct. Mater.* **2022**, *32* (48), No. 2208148.

(26) Xue, W.; Wang, J.; Huang, H.; Mei, D. Structural and Hydrolytic Stability of Coordinatively Unsaturated Metal−Organic Frameworks $M_3(BTC)_2$ (M = Cu, Co, Mn, Ni, and Zn): A Combined DFT and Experimental Study. *J. Phys. Chem. C* **2021**, *125* (10), 5832−5847.

(27) Øien-Ødegaard, S.; Bouchevreau, B.; Hylland, K.; Wu, L.; Blom, R.; Grande, C.; Olsbye, U.; Tilset, M.; Lillerud, K. P. UiO-67-type Metal-Organic Frameworks with Enhanced Water Stability and Methane Adsorption Capacity. *Inorg. Chem.* **2016**, *55* (5), 1986−1991.

(28) Tu, B.; Diestel, L.; Shi, Z. L.; Bandara, W.; Chen, Y.; Lin, W.; Zhang, Y. B.; Telfer, S. G.; Li, Q. Harnessing Bottom-Up Self-Assembly to Position Five Distinct Components in an Ordered Porous Framework. *Angew. Chem., Int. Ed.* **2019**, *58* (16), 5348−5353.

(29) Liu, L.; Konstas, K.; Hill, M. R.; Telfer, S. G. Programmed Pore Architectures in Modular Quaternary Metal-Organic Frameworks. *J. Am. Chem. Soc.* **2013**, *135* (47), 17731−17734.

(30) Liu, L.; Telfer, S. G. Systematic Ligand Modulation Enhances the Moisture Stability and Gas Sorption Characteristics of Quaternary Metal-Organic Frameworks. *J. Am. Chem. Soc.* **2015**, *137* (11), 3901−3909.

(31) Zhang, W.; Hu, Y. L.; Ge, J.; Jiang, H. L.; Yu, S. H. A Facile and General Coating Approach to Moisture/Water-Resistant Metal-Organic Frameworks with Intact Porosity. *J. Am. Chem. Soc.* **2014**, *136* (49), 16978−16981.

(32) Ding, M.; Jiang, H.-L. Improving Water Stability of Metal−Organic Frameworks by a General Surface Hydrophobic Polymerization. *CCS Chem.* **2021**, *3* (8), 2740−2748.

(33) He, T.; Kong, X. J.; Zhou, J.; Zhao, C.; Wang, K.; Wu, X. Q.; Lv, X. L.; Si, G. R.; Li, J. R.; Nie, Z. R. A Practice of Reticular Chemistry: Construction of a Robust Mesoporous Palladium Metal-Organic Framework via Metal Metathesis. *J. Am. Chem. Soc.* **2021**, *143* (26), 9901−9911.

(34) Cavka, J. H.; Jakobsen, S.; Olsbye, U.; Guillou, N.; Lamberti, C.; Bordiga, S.; Lillerud, K. P. A New Zirconium Inorganic Building Brick Forming Metal Organic Frameworks with Exceptional Stability. *J. Am. Chem. Soc.* **2008**, *130* (42), 13850−13851.

(35) Wang, T. C.; Vermeulen, N. A.; Kim, I. S.; Martinson, A. B.; Stoddart, J. F.; Hupp, J. T.; Farha, O. K. Scalable Synthesis and Post-Modification of a Mesoporous Metal-Organic Framework Called NU-1000. *Nat. Protoc.* **2016**, *11* (1), 149−162.

(36) Shi, L.; Yang, Z.; Sha, F.; Chen, Z. Design, Synthesis and Applications of Functional Zirconium-Based Metal-Organic Frameworks. *Sci. China Chem.* **2023**, *66* (12), 3383−3397.

(37) Fiankor, C.; Nyakuchena, J.; Khoo, R. S. H.; Zhang, X.; Hu, Y.; Yang, S.; Huang, J.; Zhang, J. Symmetry-Guided Synthesis of N,N'-Bicarbazole and Porphyrin-Based Mixed-Ligand Metal-Organic Frameworks: Light Harvesting and Energy Transfer. *J. Am. Chem. Soc.* **2021**, *143* (48), 20411−20418.

(38) Qiao, G. Y.; Yuan, S.; Pang, J.; Rao, H.; Lollar, C. T.; Dang, D.; Qin, J. S.; Zhou, H. C.; Yu, J. Functionalization of Zirconium-Based Metal-Organic Layers with Tailored Pore Environments for Heterogeneous Catalysis. *Angew. Chem., Int. Ed.* **2020**, *59* (41), 18224−18228.

(39) Liu, T. F.; Feng, D.; Chen, Y. P.; Zou, L.; Bosch, M.; Yuan, S.; Wei, Z.; Fordham, S.; Wang, K.; Zhou, H. C. Topology-guided Design and Syntheses of Highly Stable Mesoporous Porphyrinic Zirconium Metal-organic Frameworks with High Surface Area. *J. Am. Chem. Soc.* **2015**, *137* (1), 413−419.

(40) Ishiyama, S.; Fujii, R.; Nakamura, M.; Imahori, Y. 3 KeV H_2^+ Irradiation to Li/Pd/Cu Trilaminar Neutron Production Target for BNCT. *Mater. Trans.* **2014**, *55* (4), 658−663.

(41) Diculescu, V. C.; Beregoi, M.; Evanghelidis, A.; Negrea, R. F.; Apostol, N. G.; Enculescu, I. Palladium/palladium Oxide Coated Electrospun Fibers for Wearable Sweat pH-sensors. *Sci. Rep.* **2019**, *9*, 8092.

(42) del Cul, G. D.; Bostick, W. D.; Trotter, D. R.; Osborne, P. E. Technetium-99 Removal from Process Solutions and Contaminated Groundwater. *Sep. Sci. Technol.* **1993**, *28* (1−3), 551−564.

(43) Seliman, A. F.; Samadi, A.; Husson, S. M.; Borai, E. H.; DeVol, T. A. Preparation of Polymer-Coated, Scintillating Ion-Exchange

Resins for Monitoring of ^{99}Tc in Groundwater. *Anal. Chem.* **2011**, *83* (12), 4759−4766.

(44) Wilmarth, W. R.; Lumetta, G. J.; Johnson, M. E.; Poirier, M. R.; Thompson, M. C.; Suggs, P. C.; Machara, N. P. Review: Waste-Pretreatment Technologies for Remediation of Legacy Defense Nuclear Wastes. *Solvent Extr. Ion Exch.* **2011**, *29* (1), 1−48.

(45) Peng, H.; Jiang, B.; Li, F.; Gong, J.; Zhang, Y.; Yang, M.; Liu, N.; Ma, L. Single-Crystal-Structure Directed Predesign of Cationic Covalent Organic Polymers for Rapidly Capturing $^{99}TcO_4^-$. *Chem. Mater.* **2023**, *35* (6), 2531−2540.

(46) Sheng, D.; Zhu, L.; Dai, X.; Xu, C.; Li, P.; Pearce, C. I.; Xiao, C.; Chen, J.; Zhou, R.; Duan, T.; Farha, O. K.; Chai, Z.; Wang, S. Successful Decontamination of $^{99}TcO_4^-$ in Groundwater at Legacy Nuclear Sites by a Cationic Metal-Organic Framework with Hydrophobic Pockets. *Angew. Chem., Int. Ed.* **2019**, *58* (15), 4968−4972.

(47) Sheng, D.; Zhu, L.; Xu, C.; Xiao, C.; Wang, Y.; Wang, Y.; Chen, L.; Diwu, J.; Chen, J.; Chai, Z.; Albrecht-Schmitt, T. E.; Wang, S. Efficient and Selective Uptake of TcO_4^- by a Cationic Metal-Organic Framework Material with Open Ag^+ Sites. *Environ. Sci. Technol.* **2017**, *51* (6), 3471−3479.

(48) Zhu, L.; Sheng, D.; Xu, C.; Dai, X.; Silver, M. A.; Li, J.; Li, P.; Wang, Y.; Wang, Y.; Chen, L.; Xiao, C.; Chen, J.; Zhou, R.; Zhang, C.; Farha, O. K.; Chai, Z.; Albrecht-Schmitt, T. E.; Wang, S. Identifying the Recognition Site for Selective Trapping of $^{99}TcO_4^-$ in a Hydrolytically Stable and Radiation Resistant Cationic Metal-Organic Framework. *J. Am. Chem. Soc.* **2017**, *139* (42), 14873−14876.

(49) Zhang, D.; Ronson, T. K.; Mosquera, J.; Martinez, A.; Nitschke, J. R. Selective Anion Extraction and Recovery Using a $Fe^{II}_4L_4$ Cage. *Angew. Chem., Int. Ed.* **2018**, *57* (14), 3717−3721.

(50) Fei, H.; Bresler, M. R.; Oliver, S. R. A New Paradigm for Anion Trapping in High Capacity and Selectivity: Crystal-to-crystal Transformation of Cationic Materials. *J. Am. Chem. Soc.* **2011**, *133* (29), 11110−11113.

(51) Banerjee, D.; Xu, W.; Nie, Z.; Johnson, L. E.; Coghlan, C.; Sushko, M. L.; Kim, D.; Schweiger, M. J.; Kruger, A. A.; Doonan, C. J.; Thallapally, P. K. Zirconium-Based Metal-Organic Framework for Removal of Perrhenate from Water. *Inorg. Chem.* **2016**, *55* (17), 8241−8243.

(52) Kang, K.; Li, L.; Zhang, M.; Zhang, X.; Lei, L.; Xiao, C. Constructing Cationic Metal-organic Framework Materials Based on Pyrimidyl as a Functional Group for Perrhenate/Pertechnetate Sorption. *Inorg. Chem.* **2021**, *60* (21), 16420−16428.

(53) Xu, D.; Chen, L.; Dai, X.; Li, B.; Wang, Y.; Liu, W.; Li, J.; Tao, Y.; Wang, Y.; Liu, Y.; Peng, G.; Zhou, R.; Chai, Z.; Wang, S. A Porous Aromatic Framework Functionalized with Luminescent Iridium(III) Organometallic Complexes for Turn-On Sensing of $^{99}TcO_4^-$. *ACS Appl. Marer. Interfaces* **2020**, *12* (13), 15288−15297.

(54) Hu, Q.; Jiang, W.; Liang, R.; Lin, S.; Qiu, J. Synthesis of Imidazolium-based Cationic Organic Polymer for Highly Efficient and Selective Removal of ReO_4^-/TcO_4^-. *Chem. Eng. J.* **2021**, *419*, No. 129546.